Experimental and Theoretical Study of the Reactions between Vanadium−Silicon Heteronuclear Oxide Cluster Anions with *n*-Butane

Yan-Xia Zhao,[†,‡] Xiao-Nan Wu,[†,‡] Jia-Bi Ma,[†,‡] Sheng-Gui He,*[,†] and Xun-Lei Ding*[,†]

Beijing National Laboratory for Molecular Science (BNLMS), State Key Laboratory for Structural Chemistry of Unstable and Stable Species, Institute of Chemistry, Chinese Academy of Sciences, Beijing 100190, People's Republic of China, and Graduate School of Chinese Academy of Sciences, Beijing 100039, People's Republic of China

Received: May 18, 2010; Revised Manuscript Received: June 13, 2010

Vanadium and silicon heteronuclear oxide cluster anions $V_xSi_yO_z^-$ ($x + y \geq 2$, $z \geq 4$) are prepared by laser ablation and reacted with *n*-butane (C_4H_{10}) in a fast flow reactor. A time-of-flight mass spectrometer is used to detect the cluster distribution before and after the reactions. The observation of hydrogen-containing products $(V_2O_5)_m(SiO_2)_nOH^-$ ($m = 1$, $n = 1-4$; $m = 2$, $n = 1$) strongly suggests the following reactions: $(V_2O_5)_m(SiO_2)_nO^- + C_4H_{10} \rightarrow (V_2O_5)_m(SiO_2)_nOH^- + C_4H_9$. Although $V_2O_6^-$ is produced in the cluster source, no $V_2O_6H^-$ product is produced under the same experimental condition. It indicates that specific heteronuclear oxide clusters $V_2O_5(SiO_2)_{1-4}O^-$ and $(V_2O_5)_2SiO_2O^-$ are more reactive than the homonuclear oxide cluster $V_2O_6^-$ (or $V_2O_5O^-$). Density functional theory (DFT) calculations are performed to study reaction mechanisms of $V_2O_5SiO_2O^-$ (or $V_2SiO_8^-$) + C_4H_{10}. The calculated results are in good agreement with the experimental observations. The structural and bonding properties of $(V_2O_5)_m(SiO_2)_nO^-$ ($m = 1$, $n = 1-4$; $m = 2$, $n = 1$) are also investigated by the DFT calculations. The unpaired electron in each of the clusters is mainly distributed over one or two O atoms (2p orbitals) bonded with Si rather than V atom(s). Furthermore, the experimentally observed higher reactivity of the V−Si heteronuclear oxide cluster $(V_2O_5)_m(SiO_2)_nO^-$ over the homonuclear $V_2O_6^-$ in the reaction with C_4H_{10} is interpreted based on the theoretical results.

1. Introduction

The bonding and reactivity of gas phase homonuclear oxide clusters with different charge state have received considerable attention in recent decades, and fruitful results were obtained.[1−15] One of the interesting findings is that the existence of oxygen-centered radicals $O^{-\bullet}$ (sometimes denoted as $O^\bullet$ or O^-) of which the critical bonding character[16] is similar to gas phase and surface-absorbed O^- ions[17,18] over early transition metal oxide clusters such as $VO_3(V_2O_5)_{0-2}$,[19−21] $(V_2O_5)_{1-5}^+$,[22−25] $(ZrO_2)_{1-4}^+$,[26] and $(WO_3)_{1-3}^+$[27] is common.[28,29] In addition, some main group metal[30−33] and nonmetal oxide cluster cations[34,35] also contain $O^{-\bullet}$ radicals. Many experiments have identified that the $O^{-\bullet}$-containing clusters are very reactive toward CO and (or) hydrocarbon molecules, and the $O^{-\bullet}$ was suggested to be primarily responsible (cluster active site) for the reactions.[19,20,22−27,29−43]

These highly reactive oxide clusters may be good candidates for models of surface reactive oxygen species[44−47] that are important in various useful catalytic processes. For example, it has been demonstrated that surface $O^{-\bullet}$ species are involved in the partial oxidation of methane to methanol and formaldehyde by nitrous oxide over silica-supported vanadium and molybdenum oxides.[48−53] Note that $O^{-\bullet}$ species over oxides may be generated through photoirradiation (and electron/hole separation), adsorption, and dissociation of O_2 and N_2O, and other surface chemical interactions. The chemistry of surface-adsorbed $O^{-\bullet}$ species has been widely studied by electron spin resonance/electron paramagnetic resonance spectroscopy,[18,49,54] while the cluster study may reveal further structural and reactivity properties. It should be pointed out that practical materials are usually overall neutral, while a specific site over the surface may be positively or negatively charged through charge transfer, so it is important to study oxide clusters in different charge states (neutrals, cations, and anions).[29]

The metal oxide catalysts are usually supported on or mixed with other materials in heterogeneous catalytic reactions. For example, vanadium oxides supported on porous SiO_2,[55] Al_2O_3,[56] TiO_2,[57] ZrO_2,[58] and CeO_2[59] have been extensively used as catalytic materials in selective oxidation of light alkanes,[60−62] alcohol,[63,64] sulfides,[65] and olefins.[66] It is useful to study the gas phase heteronuclear oxide clusters such as $V_xSi_yO_z^{0,\pm1}$ to interpret chemical structures and reactivity of the interface between active phase and support material in metal oxide-based catalysts such as V_2O_5/SiO_2.

In contrast to the extensive studies of homonuclear oxide clusters, heteronuclear oxide clusters are much less studied,[67,68] and several valuable results were only reported recently.[68,69] An experimental study indicated that the bimetallic oxide cluster $AlVO_4^+$ can abstract a hydrogen atom from CH_4 at near room temperature conditions, and density functional theory (DFT) calculations identified that the $O^{-\bullet}$ radical in $AlVO_4^+$ is bonded with the Al rather than the V atom.[69] The DFT studies also predicted that $TiVO_5$ and $CrVO_6$[28] and $ZrScO_4$ and $ZrNbO_5$[68] contain $O^{-\bullet}$ radicals. The geometric and electronic structure of bimetallic oxide clusters $(V_2O_5)_{1-3}(VTiO_5)^-$ and $V_{4-i}Ti_iO_{10}^-$ ($i = 1-4$) were studied by infrared multiple photodissociation spectroscopy and theoretical calculations.[70]

In this study, we focus on the structural and reactivity properties of the vanadium−silicon heteronuclear oxide cluster anions $V_xSi_yO_z^-$. Several experimental studies on the reactivity of the homonuclear vanadium oxide clusters toward hydrocarbon

* To whom correspondence should be addressed. Tel: 86-10-62536990. Fax: 86-10-62559373. E-mail: shengguihe@iccas.ac.cn (S.-G.H.) or dingxl@iccas.ac.cn (X.-L.D.).
† Chinese Academy of Sciences.
‡ Graduate School of Chinese Academy of Sciences.

10.1021/jp1045244
Published on Web 06/29/2010

molecules established that $V_xO_z^-$ clusters anions[71,72] are usually inert or only display minor reaction channels at room temperature, while the $V_xO_z^+$ cations[23,24,71−75] are generally much more reactive. It was interpreted that the presence of the positive charge may act to strengthen the interaction with hydrocarbons and enhance the effect of electron withdrawal. However, the negative charge will reduce electron-withdrawing effects and less strongly polarize hydrocarbons.[76] The studies of vanadium oxide cluster anions were mostly concentrated on the geometric structure and photoelectron spectroscopy,[9,77−83] while the reactivity is much less studied.[84−86] It is interesting to study if the reactivity of $V_xO_z^-$ can be tuned or enhanced by doping or mixing silicon (Si) atom(s) to form $V_xSi_yO_z^-$ cluster anions.

2. Methods

2.1. Experimental Methods. The experimental setup for a pulsed laser ablation/supersonic nozzle coupled with a fast flow reactor was similar to the one described in previous studies.[4,19,87] Only a brief outline of the experiments is given below. The V−Si heteronuclear oxide anions $V_xSi_yO_z^-$ were created in a narrow cluster formation channel (2 mm diameter × 25 mm length) by the reaction of laser ablation-generated vanadium and silicon plasmas with 1% O_2 seed in the helium (99.999% purity) carrier gas with a backing pressure of 5 atm. To generate the V/Si plasmas, a 532 nm (second harmonic Nd^{3+}:YAG, 5 mJ/pulse, 8 ns duration, 10 Hz repetition rate) laser was focused onto a translating and rotating V/Si mixed powder disk (mole ratio of V:Si = 1:1) that exposes a fresh surface continually. The gas was controlled by a pulsed valve (General Valve, Series 9). To eliminate the water impurity that often occurs in the cluster distribution, the prepared gas mixture (O_2/He, denoted as the cluster generation gas) was passed through a 10 m long copper tube coil at low temperature ($T = 77$ K) before entering into the pulsed valve. Similar treatment ($T = 263$ K) was also applied in the use of the reactant gases (see below).

The generated oxide anions $V_xSi_yO_z^-$ were expanded and reacted with reactant gases (C_4H_{10}/C_4D_{10}) in a fast flow reactor (6 mm diameter × 60 mm length). The reactant gases with backing pressures of 2−15 kPa were pulsed into the reactor 20 mm downstream from the exit of the narrow cluster formation channel by a second pulsed valve (General Valve, Series 9). The instantaneous total gas pressure in the fast flow reactor was estimated to be around 300 Pa at $T = 350$ K. The cluster vibrational temperature was assumed to be close to the carrier gas temperature, which was around 300−400 K, considering that the gas can be heated during the process of laser ablation. After they were reacted in the fast flow reactor, the reactant and product ions exiting from the reactor were skimmed (3 mm diameter) into a vacuum system of a time-of-flight mass spectrometer (TOF-MS) for mass (to charge ratio) measurement. Ion signals were generated by a dual microchannel plate detector and recorded with a digital oscilloscope (LeCroy WaveSurfer 62Xs) by averaging 500−1000 traces of independent mass spectra (each corresponds to one laser shot). The uncertainty of the reported relative ion signals was about 10%. The mass resolution was about 400−500 ($M/\Delta M$) with the current experimental setup. It was noticeable that the ionic metal oxide clusters could be mass selected and trapped in or passed through a gas cell for the reactivity studies as demonstrated by several research groups.[23,26,88,89] The fast flow reaction method[90] adopted in this study was relatively simple and did not have the capability to mass select a cluster before the reaction. However, both the hydrogen atom abstraction (such as $M_xO_z^{\pm} + C_pH_q \rightarrow M_xO_zH^{\pm} + C_pH_{q-1}$)[25,87] and the oxygen atom transfer reactions (such as $M_xO_z^{\pm} + C_pH_q \rightarrow M_xO_{z-1}^{\pm} + C_pH_qO$)[87] that are attractive processes in terms of catalysis could be identified by such a simple method. In the latter case, the TOF mass peak of $M_xO_{z-1}^{\pm}$ from the reaction would overlap with that of $M_xO_{z-1}^{\pm}$ from the cluster source, while one could observe the signal increase of $M_xO_{z-1}^{\pm}$ upon the reaction.[87] An appropriate choice of O_2 concentration in the generation of the clusters to make relatively higher abundance of $M_xO_z^{\pm}$ versus that of $M_xO_{z-1}^{\pm}$ was also important to identify the oxygen atom transfer processes in the fast flow reaction experiments.

2.2. Computational Methods. The DFT calculations using the Gaussian 03 program[91] were employed to study the geometric structures of reactive heteronuclear oxide cluster anions $(V_2O_5)_m(SiO_2)_nO^-$ ($m = 1$, $n = 1-4$; $m = 2$, $n = 1$) and the reaction mechanism of selected $(V_2O_5)_m(SiO_2)_nO^-$ clusters toward C_4H_{10}. To understand the bonding property of the saturated V−Si heteronuclear oxide anions, the geometry optimizations were performed starting from a high number of possible candidate structures based on chemical intuition. All possible spin multiplicities for each geometry were also tested to find the most stable electronic state. For the smallest heteronuclear cluster anion $V_2O_5SiO_2O^-$ (or $V_2SiO_8^-$), it was quite certain that the lowest energy structure was obtained. For larger clusters, especially $V_2O_5(SiO_2)_4O^-$ (or $V_2Si_4O_{14}^-$) and $(V_2O_5)_2SiO_2O^-$ (or $V_4SiO_{13}^-$), although many candidate structures were tried and the possible low-lying energy isomers were proposed, the most promising approach such as genetic algorithm[31] may be necessary to find global minimum structures. All structures presented in this paper were fully optimized, and vibrational frequency analysis was performed to ensure that the optimized geometries were minima. To study the bonding properties, natural bond orbital (NBO) analyses were performed using NBO 3.1[92] implemented in Gaussian 03.

The reaction mechanism calculations involved geometry optimizations of various reaction intermediates and transition states (TSs) through which the intermediates transferred to each other. The TS optimizations were performed by using the Berny algorithm.[93] The initial guess structure of the TS species was obtained through relaxed potential energy surface scans using an appropriate internal coordinate. Vibrational frequency calculations were performed to check that reaction intermediates and TS species had zero and one imaginary frequency, respectively. Intrinsic reaction coordinate calculations[94,95] were also performed so that a TS connected two appropriate local minima in the reaction pathways. The hybrid B3LYP exchange correlation functional[96−98] in combination with all-electron polarized triple-ζ valence basis sets (TZVP)[99] were used for V, Si, O, C, and H atoms throughout this work. Test calculations indicated that basis set superposition error (BSSE)[100,101] was negligible, so the BSSE was not taken into consideration in this study. The calculated energies reported in this study were the relative zero-point vibration corrected (ΔH_{0K}) and Gibbs free energies (ΔG_{298K}).

3. Results

3.1. Experimental Results. ***3.1.1. $V_xSi_yO_z^-$ Cluster Generation.*** Figure 1a presents a typical TOF mass spectrum for the distribution of $V_xSi_yO_z^-$ ($x + y = 2-6$, $4 \le z \le 13$) clusters generated under the condition of 1% O_2 seeded in 5 atm He. Oxygen slightly deficient clusters $VO_2(SiO_2)_{2-5}^-$, $V_2O_5(SiO_2)_{1-4}^-$, $(V_2O_5)VO_2(SiO_2)_{2,3}^-$, and $(V_2O_5)_2SiO_2^-$ with relatively high abundance are produced in $VSi_yO_z^-$ ($y = 2-5$, $z = 5-13$), $V_2Si_yO_z^-$ ($y = 1-4$, $z = 5-14$), $V_3Si_{2,3}O_z^-$ ($z = 10-13$), and $V_4SiO_z^-$ ($z = 11-13$) series, respectively. Meanwhile, oxygen-

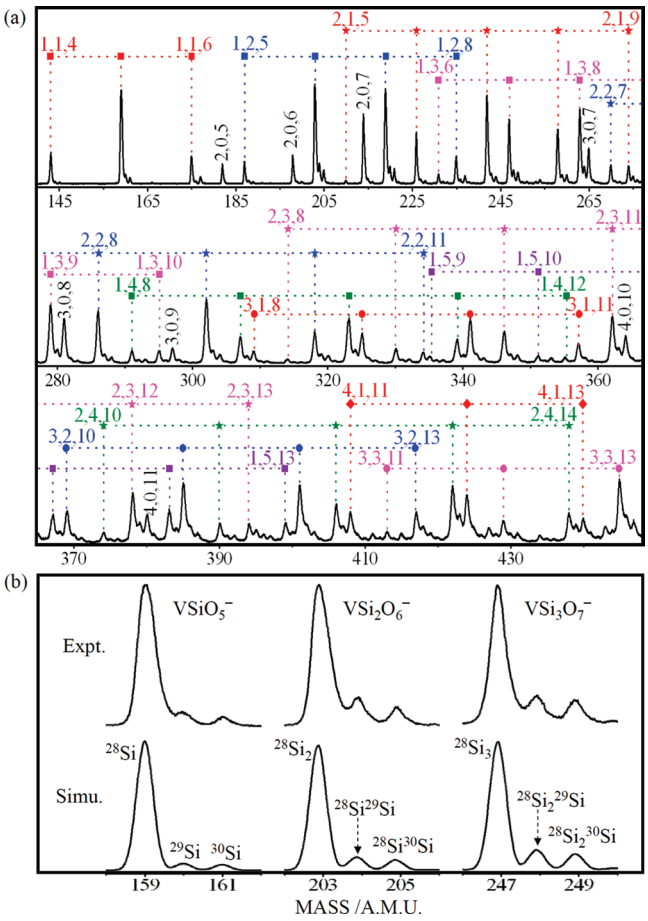

Figure 1. TOF mass spectra for the distribution of V−Si heteronuclear oxide cluster anions $V_xSi_yO_z^-$ (a). Cluster series with $x = 1$, 2, 3, and 4 are marked by a square, asterisk, circle, and diamond, respectively, and $V_xSi_yO_z^-$ clusters are denoted as x,y,z. The experimental and simulated isotopic patterns for $VSiO_5^-$, $VSi_2O_6^-$, and $VSi_3O_7^-$ isotopomers are shown in panel b.

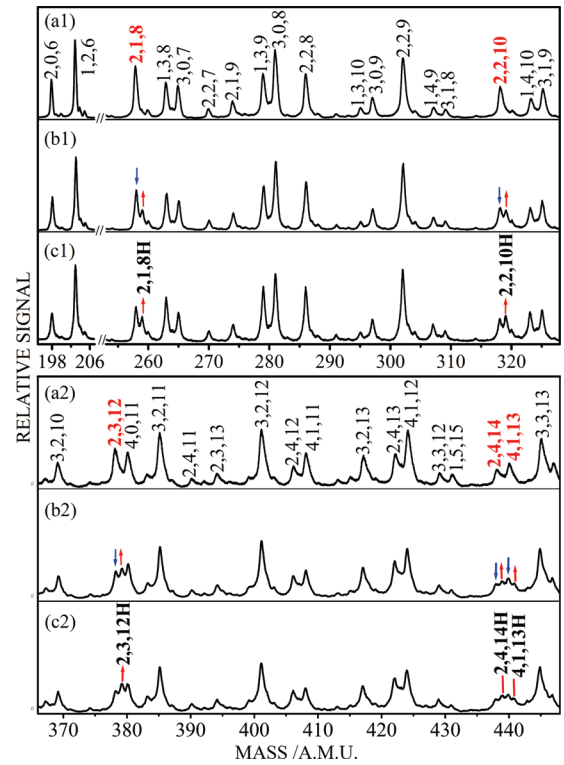

Figure 2. TOF mass spectra for reactions of $V_xSi_yO_z^-$ clusters with (a) He gas (for reference), (b) 2 Pa of C_4H_{10}, and (c) 3 Pa of C_4H_{10} in the fast flow reactor. The $V_xSi_yO_z^-$ and $V_xSi_yO_zH^-$ clusters are denoted as x,y,z and x,y,zH, respectively.

saturated clusters $VO_3SiO_2^-$ and $(V_2O_5)VO_3SiO_2^-$ with relatively high abundance are produced in $VSiO_z^-$ ($z = 4-6$) and $V_3SiO_z^-$ ($z = 8-11$) clusters, respectively. In addition to V−Si heteronuclear oxide anions, several homonuclear vanadium oxide anions $V_2O_{5-7}^-$, $V_3O_{7-9}^-$, and $V_4O_{10-11}^-$ are also generated, but no apparent signals of homonuclear silicon oxide anions $Si_yO_z^-$ are observed in this case. Silicon has three stable isotopes: ^{28}Si (92.23%), ^{29}Si (4.67%), and ^{30}Si (3.10%). The isotopomers originated from Si_y ($y \geq 1$) for mass signals of V−Si heteronuclear oxide anions can be resolved by the mass spectrometer. Portions of the experimental mass spectra for $V_xSi_yO_z^-$ clusters containing one, two, and three Si atoms (Si, Si_2, and Si_3) are replotted and compared with the simulated patterns of the corresponding isotopomers in Figure 1b. There is a good agreement between the experiment and the simulation.

3.1.2. Reactions of $V_xSi_yO_z^-$ Clusters with C_4H_{10}. The TOF mass spectra for reactions of $V_xSi_yO_z^-$ clusters with C_4H_{10} are plotted in Figure 2. When a low concentration of C_4H_{10} (2 Pa) is pulsed into the fast flow reactor, the signal magnitudes of $V_2O_5SiO_2O^-$ (or $V_2SiO_8^-$), $V_2O_5(SiO_2)_2O^-$ (or $V_2Si_2O_{10}^-$), $V_2O_5(SiO_2)_3O^-$ (or $V_2Si_3O_{12}^-$), $V_2O_5(SiO_2)_4O^-$ (or $V_2Si_4O_{14}^-$), and $(V_2O_5)_2SiO_2O^-$ (or $V_4SiO_{13}^-$) decrease, while five new products, which can be assigned as $V_2O_5(SiO_2)_{1-4}OH^-$ and $(V_2O_5)_2SiO_2OH^-$, are produced upon the reaction. In sharp contrast, the signal magnitudes of all of the other clusters are almost kept. Note that no association products $V_xSi_yO_zC_4H_{10}^-$ can be observed. With the increase of the C_4H_{10} pressure (3 Pa), the mass signals of products generally become relative more intense. The results in Figure 2 strongly suggest that the hydrogen atom abstraction reactions take place in the fast flow reactor as follows:

$$(V_2O_5)_m(SiO_2)_nO^- + C_4H_{10} \rightarrow (V_2O_5)_m(SiO_2)_nOH^- + C_4H_9 \quad (1)$$

in which $m = 1$, $n = 1-4$ and $m = 2$, $n = 1$. Isotopic labeling experiments further confirm the above reactions. For example, the products $V_2O_5SiO_2OD^-$ (or $V_2SiO_8D^-$) and $V_2O_5(SiO_2)_2OD^-$ (or $V_2Si_2O_{10}D^-$) are produced in the cluster reaction with C_4D_{10} as shown in Figure S1 in the Supporting Information.

The experimental results demonstrate that V−Si heteronuclear oxide anions $V_2O_5(SiO_2)_{1-4}O^-$ and $(V_2O_5)_2SiO_2O^-$ exhibit reactivity toward C_4H_{10}, whereas the homonuclear oxide cluster $V_2O_6^-$ (or $V_2O_5O^-$) does not (see the mass spectra around 198 amu region in Figure 2). The first order rate constant (k_1) in the fast flow reactor can be estimated by $I = I_0 \exp(-k_1\rho\,\Delta t)$, in which I and I_0 are signal magnitudes of the clusters in the presence and absence of reagent gas (C_4H_{10}), respectively; ρ is the molecular density of reactant gas (the method to calculate ρ has been described in ref 4); and Δt is the effective reaction time (~60 μs). The estimated rate constants of $k_1(V_2O_5SiO_2O^- + C_4H_{10})$, $k_1[V_2O_5(SiO_2)_2O^- + C_4H_{10}]$, $k_1[V_2O_5(SiO_2)_3O^- + C_4H_{10}]$, $k_1[V_2O_5(SiO_2)_4O^- + C_4H_{10}]$, and $k_1[(V_2O_5)_2SiO_2O^- + C_4H_{10}]$ are 2.0×10^{-11}, 2.8×10^{-11}, 3.3×10^{-11}, 3.5×10^{-11}, and 2.3×10^{-11} cm^3 molecule^{-1} s^{-1}, respectively. The uncertainties for the relative rate constants are within 20%, while the absolute values may vary by a factor of 5 due to systematic deviations in the estimation of the reactant gas pressures (ρ) and reaction time (Δt) in the experiments.

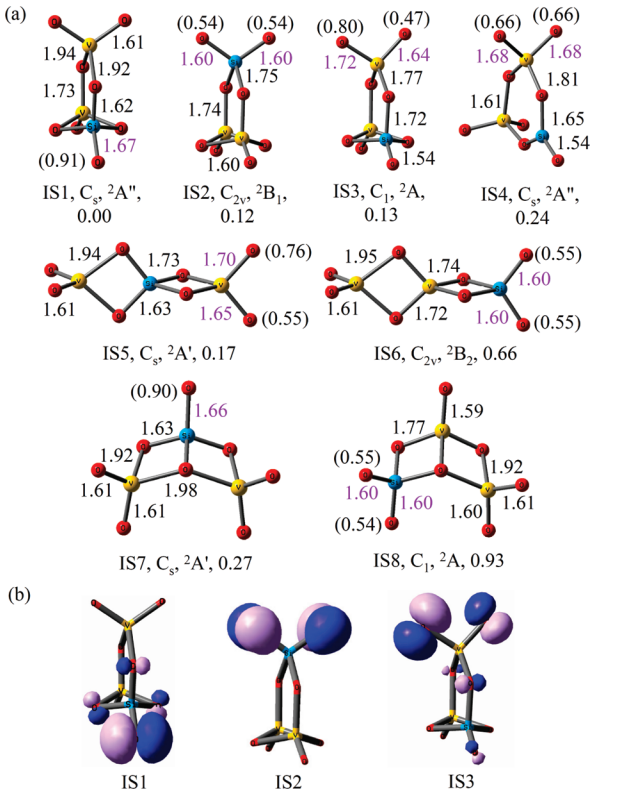

Figure 3. DFT calculated isomeric structures of $V_2O_5SiO_2O^-$ (a). The symmetry, electronic state, relative energy (in eV), and bond lengths (in Å) are given for each structure. The Mulliken spin density values in |e| over oxygen atoms are given in the parentheses. The SOMOs of IS1−IS3 are shown in panel b.

3.2. Computational Results. ***3.2.1. Consideration of the Computational Accuracy.*** A hybrid B3LYP functional in combination with TZVP basis set has been extensively used to give reasonably good results at moderate computational costs for geometric and reactive properties of homonuclear vanadium oxide systems.[9,19−21,23,24,73,77−81,85,102,103] The same method was also used to model the reactions that occurred at silicon-supported vanadia, and good agreement between calculations and experiments was also obtained.[104−108] In this study, test calculations of bond dissociation energy (D_e), vertical ionization energy (IE_v), adiabatic electron affinity (EA_{ad}), and adiabatic and (or) vertical detachment energy (VDE) for silicon oxides along with related molecules are performed employing hybrid B3LYP functional coupled with TZVP basis set. The calculated and available experimental values[109−118] are listed in Table S1 in the Supporting Information. It can be seen that most of the computed results for silicon species agree with the experimental values very well, especially for the VDE of SiO_2^-. It concludes that the B3LYP/TZVP method can give reasonably good results for the bonding and reactivity properties of vanadium−silicon heteronuclear oxide clusters.

3.2.2. Structures of the $V_2O_5SiO_2O^-$ Cluster. The geometric structures of the smallest cluster $V_2O_5SiO_2O^-$ (or $V_2SiO_8^-$) in eq 1 are carefully studied so that it is certain that the global minimum is obtained. Figure 3 displays the B3LYP optimized isomeric structures for $V_2O_5SiO_2O^-$ with energies less than 1 eV. The information for bond lengths and the distributions of Mulliken spin densities is also given.

These isomers are all doublet. IS1 (C_s, $^2A''$), IS2 (C_{2v}, $^2B_1$), and IS3 (C_1, ^2A) are close in energy (within 0.13 eV). They have very similar topological structures. Each of the X atoms (X = Si and V) in IS1−IS3 are fourfold coordinated with oxygen atoms to form either $O_tX(O_b)_3$ or $(O_t)_2X(O_b)_2$ building blocks, in which O_b and O_t represent bridging and terminal oxygen atoms, respectively. Spin density distribution analysis shows that the spin density of IS1 is mainly localized at a single O_t atom (0.91 |e|) with an elongated Si−O_t bond (1.67 Å, the Wiberg bond order is 0.76), which is 0.15 Å longer than the Si═O double bond in SiO_2 molecule (1.52 Å by B3LYP). It indicates that the terminal oxygen atom O_t with most of the spin density values (such O_t atom is denoted as $O_t^\bullet$ in the text below) in $V_2O_5SiO_2O^-$ can be viewed as an $O^{-\bullet}$ radical. Accordingly, the moiety $(O_b)_3SiO_t$ in IS1 can be described as $(O_b)_3SiO_t^\bullet$. Both IS2 and IS3 have spin densities distributed over two O_t atoms that can be described as $(O_b)_2Si(O_tO_t)^\bullet$ (0.54/0.54 |e|) and $(O_b)_2V(O_tO_t)^\bullet$ (0.80/0.47 |e|), respectively. The singly occupied molecular orbitals (SOMOs, the MOs are the Kohn−Sham orbitals with DFT) of the three most stable isomers are shown in Figure 3b. It can be seen that each of the SOMOs is localized on one or two terminal oxygen atoms, which is consistent with the spin density distributions discussed above, and all of the SOMOs are with character of O 2p orbitals.

The isomers with $X(O_b)_4$ moiety (IS5 and IS6), 3-fold coordinated X atoms (IS4), or 3-fold O atoms (IS7 and IS8) are all higher in energy than IS1−IS3, and they also have $(O_b)_3SiO_t^\bullet$, $(O_b)_2V(O_tO_t)^\bullet$, or $(O_b)_2Si(O_tO_t)^\bullet$ moieties, respectively. The relative energetics suggest that for the clusters with similar topological structures, isomers with $(O_b)_3SiO_t^\bullet$ or $Si(O_b)_4$ moieties are more stable than the ones with $(O_b)_2X(O_tO_t)^\bullet$ or $V(O_b)_4$, respectively.

3.2.3. Reaction Mechanisms of $V_2O_5SiO_2O^-$ + C_4H_{10}. To gain insight into the mechanistic details of hydrogen atom abstraction from C_4H_{10} by $V_2O_5SiO_2O^-$, reaction mechanisms for the two possible reaction channels involved with IS1 are studied by the DFT calculations:

$$V_2O_5SiO_2O^-\ (IS1) + C_4H_{10} \rightarrow V_2O_5SiO_2OH^- + 2\text{-}C_4H_9 \qquad \Delta H_{0K} = -0.97\ eV \quad (2)$$

$$V_2O_5SiO_2O^-\ (IS1) + C_4H_{10} \rightarrow V_2O_5SiO_2OH^- + 1\text{-}C_4H_9 \qquad \Delta H_{0K} = -0.79\ eV \quad (3)$$

Both of the hydrogen atom abstraction channels are exothermic. The potential energy profile for reaction 2 is plotted in Figure 4. The structures and energies of the reaction intermediates and TSs are also given. When C_4H_{10} approaches IS1, an encounter complex IM1 with a binding energy of 0.15 eV (ΔH_{0K} value) exists. In IM1, one hydrogen atom (H1) interacts with the radical center $O_t^\bullet$ (O1) through weak hydrogen bonding, and the O1−H1 distance is 2.62 Å. Then, the reaction proceeds by a TS TS1. It is noticeable that TS1 can be considered as an early TS[33] because the O1−H1 distance is 1.88 Å, which is quite long, and there is no significant bonding between O1 and H1 atoms. If the zero-point energy (ZPE) correction is not taken into account, the energy of TS1 is slightly higher (by ca. 0.01 eV) than that of the IM1. The TS1 is below IM1 by 0.01 eV when the ZPE is included. In IM2, the O1−H1 bond interacts with the 2-butyl moiety weakly, and IM2 can easily dissociate into $V_2SiO_8H^-$ and 2-C_4H_9. For reaction channel 3, the C−H bond activation is subject to an overall barrier of 0.02 eV. Both the thermodynamic and the kinetic factors favor the secondary C−H bond (methylene group) activation of C_4H_{10} by the $V_2O_5SiO_2O^-$ cluster.

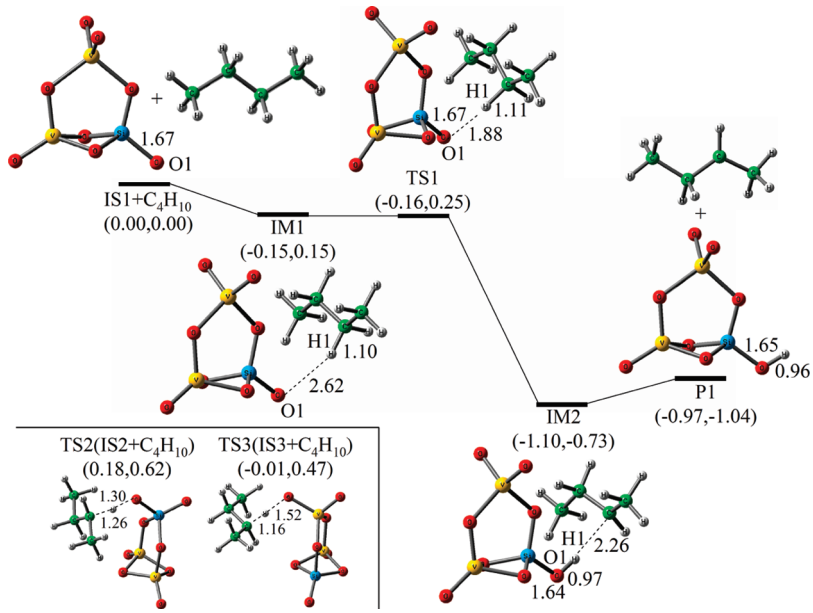

Figure 4. DFT calculated reaction pathway for $V_2O_5SiO_2O^-$ (IS1) + C_4H_{10} → $V_2O_5SiO_2OH^-$ + 2-C_4H_9. The TS structures for the reactions of $V_2O_5SiO_2O^-$ (IS2 and IS3) with C_4H_{10} are also given in the left-bottom panel, and they are denoted as TS2 and TS3, respectively. The ΔH_{0K}/ΔG_{298K} values with respect to the entrance channel of the reaction in eV are given in the parentheses. Some critical bond lengths in Å are given.

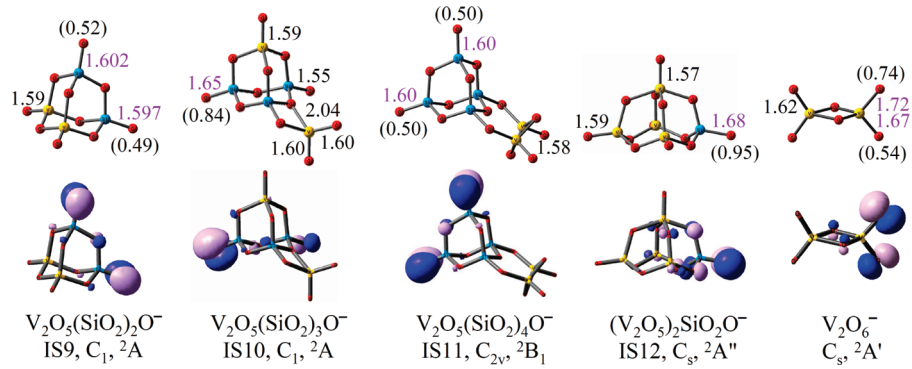

Figure 5. DFT calculated structures and SOMOs of the lowest energy isomers of $V_2O_5(SiO_2)_2O^-$ (IS9), $V_2O_5(SiO_2)_3O^-$ (IS10), $V_2O_5(SiO_2)_4O^-$ (IS11), and $(V_2O_5)_2SiO_2O^-$ (IS12). The results of $V_2O_6^-$ are also shown for comparison. The symmetry, electronic state, and bond lengths (in Å) are given for each structure. Mulliken spin density values (in |e|) over oxygen atoms are given in parentheses.

The IS1, IS2, and IS3 of $V_2SiO_8^-$ in Figure 3 are energetically competitive isomers. The hydrogen abstraction pathways for IS2/C_4H_{10} and IS3/C_4H_{10} systems are also computed, and the optimized TS structures (TS2 for IS2/C_4H_{10}; TS3 for IS3/C_4H_{10}) are shown in the left-bottom side of Figure 4. The relative energies of TS2 and TS3 for the C−H activation are 0.18 and −0.01 eV, respectively. Considering the fact that the reaction rate of $V_2SiO_8^-$ + C_4H_{10} is fast ($k_1 = 2.0 \times 10^{-11}$ cm^3 molecule^{-1} s^{-1}) and the C−H activation by the IS1 is the easiest, we conclude that the lowest energy structure IS1 by B3LYP is likely the global minimum.

3.2.4. Larger $(V_2O_5)_m(SiO_2)_nO^-$ ($m = 1$, $n = 2-4$; $m = 2$, $n = 1$) Clusters. The obtained lowest energy structures and the SOMOs of $V_2O_5(SiO_2)_{2-4}O^-$ and $(V_2O_5)_2SiO_2O^-$ are displayed in Figure 5. It can be seen that each of these cluster isomers also has one (or equivalently one) $O_t^\bullet$ atom bonded with Si rather than V (see Figures S2−S5 in the Supporting Information for various higher energy isomers for these clusters).

IS9 of $V_2O_5(SiO_2)_2O^-$ (or $V_2Si_2O_{10}^-$) is C_1 symmetry and composed of $O_tX(O_b)_3$ (X = Si or V) building blocks. One of the Si−O_t bonds (1.602 Å) is slightly longer than the other Si−O_t bond (1.597 Å) in IS9. When the C_1 symmetry of IS9 is restricted to C_s or C_2, the optimized structures always have imaginary vibrational frequencies. The alternative isomers of $V_2O_5(SiO_2)_2O^-$ (Figure S2 in the Supporting Information) are all significantly higher in energy (>1.2 eV) than the IS9 with a cage structure, indicating a high stability of the cage. In the IS10 or IS11 there is also a cage moiety topologically similar to the one of IS9. The IS12 is also a cage structure with one $O_tV(O_b)_4$ and four $O_tX(O_b)_3$ building blocks. For $V_2O_5(SiO_2)_3O^-$ (or $V_2Si_3O_{12}^-$), IS26 (Figure S3 in the Supporting Information) is only higher in energy than IS10 by 0.04 eV and for $(V_2O_5)_2SiO_2O^-$ (or $V_4SiO_{13}^-$), IS12, IS67, and IS68 (Figure S5 in the Supporting Information) are also very close in energy. It is noticeable that all of these low-lying energy isomers have the bonding character of Si−$O_t^\bullet$ rather than V−$O_t^\bullet$.

The prediction of existence of Si−$O_t^\bullet$ rather than V−$O_t^\bullet$ in the heteronuclear oxide clusters $(V_2O_5)_m(SiO_2)_nO^-$ gives a quick interpretation of the experimental results that $(V_2O_5)_m(SiO_2)_nO^-$ ($m = 1$, $n = 1-4$; $m = 2$, $n = 1$) can abstract a hydrogen atom from C_4H_{10}, while $V_2O_6^-$ (or $V_2O_5O^-$) with V−$O_t^\bullet$ can not under the same reaction conditions (Figure 2). This also indicates that the so far obtained lowest energy isomers IS9−IS12 in Figure 5 for larger clusters are the candidates of the true ground states, although further computations using special method such as genetic algorithm[31] may be necessary to find the global minima

structure at the B3LYP level of theory. The bonding of the anions may be further studied by photoelectron spectroscopy. The DFT predicts that the VDE values of IS1 and IS9−IS12 are 6.05, 5.66, 6.44, 5.86, and 7.28 eV, respectively.

4. Discussion

4.1. $\Delta = 1$ Clusters. The studies[19,20,25−38,41−43] of the bonding and reactivity of early transition metal oxide clusters $M_xO_z^{0,\pm1}$ (M in groups 3−7) indicated that most of the clusters with $\Delta \equiv 2z - nx + q = 1$, in which n is the number of metal valence electrons and q is the charge number, have the character of oxygen-centered radical $O^{-\bullet}$. It should be pointed out that the relationship of the number of valence electrons (V/5, Si/4, and O/2) and charge state ($q = -1$) of the reactive V−Si heteronuclear oxide cluster anions $V_{x1}Si_{x2}O_z^q$ [$= V_2O_5(SiO_2)_{1-4}O^-$ and $(V_2O_5)_2SiO_2O^-$] exactly meets a similar expression $\Delta \equiv 2z - (n_1x_1 + n_2x_2) + q = 1$, in which n_1 and n_2 are the numbers of the valence electrons of the V and Si atoms, respectively. A similar situation occurs for V−Al bimetallic oxide cluster cation $AlVO_4^+$ that has one $O_t^\bullet$ atom and can abstract a hydrogen atom from methane.[69] On the basis of the expression of $\Delta \equiv 2z - \sum n_i x_i + q = 1$, one can quickly judge what kind of heternuclear oxide clusters may contain mono-oxygen-centered radical. These $\Delta = 1$ clusters may be particularly oxidative toward CO and (or) hydrocarbon molecules according to the literature reports[19,20,25−27,29−38,41−43,119] as well as this study. Note that the oxygen more-rich clusters ($\Delta = 2$, 3, ...) such as $V_2SiO_9^-$, $V_2Si_2O_{11}^-$, $V_2Si_3O_{13}^-$, and so on (Figure 2) may be peroxo or superoxo species, and they are usually inert or much less oxidative than the $\Delta = 1$ series in the reaction with hydrocarbon molecules.

4.2. Comparing the Reactivity of $V_2O_5(SiO_2)_{1-4}O^-$ and $(V_2O_5)_2SiO_2O^-$ with $V_2O_6^-$. Figure 2 indicates $V_2O_6^-$ is produced, while no $V_2O_6H^-$ is observed in the reaction with C_4H_{10}. Thus, homonuclear oxide cluster $V_2O_6^-$ (or $V_2O_5O^-$) is much less reactive than heteronuclear oxide clusters $V_2O_5(SiO_2)_{1-4}O^-$ and $(V_2O_5)_2SiO_2O^-$. The study of the C−H bond activation by $M_jO_{2j}^+$ (M = Ce and Zr)[87] proposed that the reactivity of the $O_t^\bullet$ radicals in $M_jO_{2j}^+$ can be efficiently tuned by the amount of spin densities over the O_t atom that interacts directly with the C−H σ bond. This statement can rationalize that $V_2O_5SiO_2O^-$, $V_2O_5(SiO_2)_3O^-$, and $(V_2O_5)_2SiO_2O^-$ are more reactive than $V_2O_6^-$, since the SOMOs of these three V−Si heteronuclear oxide cluster anions are mainly localized at a single O_t atom (Mulliken spin density values 0.84−0.95 |e|), while the SOMO of $V_2O_6^-$ is mainly distributed over two O_t atoms (0.74 and 0.54 |e|, see Figure 5).[28]

Figure 5 indicates that $V_2O_5(SiO_2)_2O^-$ (IS9) or $V_2O_5(SiO_2)_4O^-$ (IS11) has spin densities localized over two O_t atoms, which is similar to the situation of $V_2O_6^-$. However, Figure 2 shows that $V_2O_5(SiO_2)_2O^-$ (or $V_2Si_2O_{10}^-$) and $V_2O_5(SiO_2)_4O^-$ (or $V_2Si_4O_{14}^-$) are much more reactive than $V_2O_6^-$. To interpret this result, the thermodynamic and kinetic factors are considered for the following reaction channels:

$$V_2O_5(SiO_2)_2O^-\ (IS9) + C_4H_{10} \rightarrow V_2O_5(SiO_2)_2OH^- + 2\text{-}C_4H_9 \quad \Delta H_{0K} = -0.87\ eV \quad (4)$$

$$V_2O_6^- + C_4H_{10} \rightarrow V_2O_6H^- + 2\text{-}C_4H_9 \quad \Delta H_{0K} = -0.50\ eV \quad (5)$$

The structures of the TSs (TS4 for reaction 4 and TS5 for reaction 5) involved with the C−H activation are optimized and

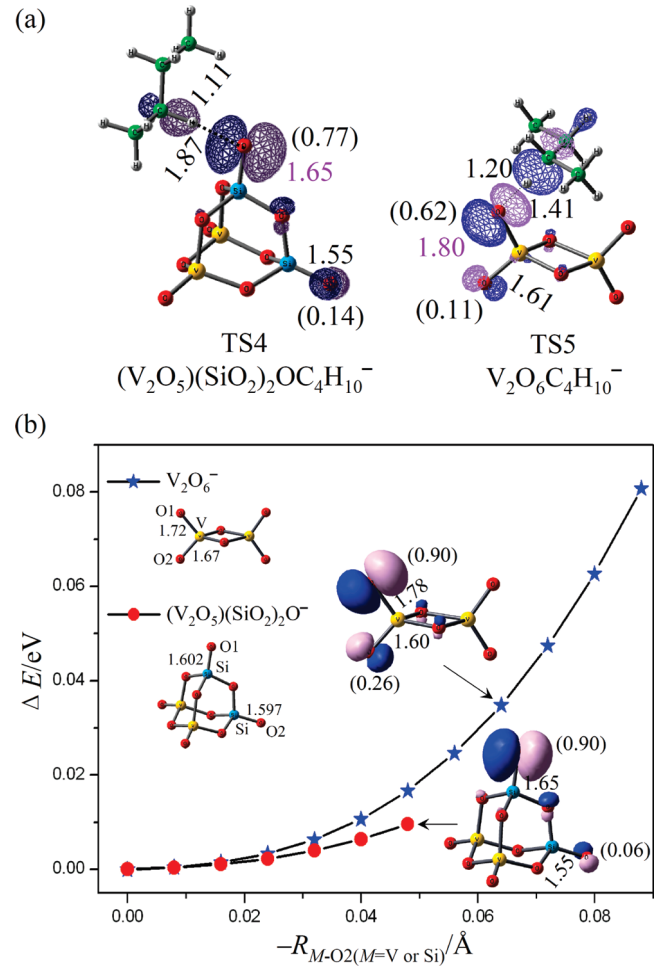

Figure 6. DFT calculated structures and SOMOs for the TSs involved with $V_2O_5(SiO_2)_2O^- + C_4H_{10}$ and $V_2O_6^- + C_4H_{10}$ (a). The Mulliken spin density values (in unit of |e| in the parentheses) over oxygen atoms and some bond lengths (in Å) are given. Panel b shows the relaxed potential energy curves obtained by shortening the Si−O2 and V−O2 bond lengths to a series of values and optimizing all of the other vibrational degrees of freedom in $V_2O_5(SiO_2)_2O^-$ (IS9) and $V_2O_6^-$ clusters, respectively.

shown in Figure 6a. The energies (ΔH_{0K}) of TS4 and TS5 with respect to the corresponding separated reactants are −0.04 and 0.01 eV, respectively. As a result, reaction 4 is both thermodynamically and kinetically more favorable than reaction 5, which is consistent with the experimental result.

In the process of C−H σ bond activation by the $O_t^\bullet$-containing clusters, electron transfer or spin density redistribution occurs to make significant touch or overlap between the $O_t^\bullet$ 2p and the C−H σ orbital.[87] Figure 6a shows that the spin densities originally distributed in the *spare* $O_t^\bullet$ atoms (that do not interact directly with C_4H_{10}, see Figures 5 and 6a) are transferred to the *touching* area between the clusters and the C_4H_{10} molecule and the lengths of the *spare* Si−$O_t^\bullet$ and V−$O_t^\bullet$ bonds are significantly shortened. Figure 6b shows the relaxed potential energy curves by shortening the spare Si−$O_t^\bullet$ and V−$O_t^\bullet$ bond lengths to a series of values and optimizing all of the other vibrational degrees of freedom in $V_2O_5(SiO_2)_2O^-$ (IS9) and $V_2O_6^-$ clusters, respectively. It indicates that the spin density transfer and localization are more facile in $V_2O_5(SiO_2)_2O^-$ (IS9) than in $V_2O_6^-$. For example, to have spin density values of 0.90 |e| being localized over the reacting Si−$O_t^\bullet$ and V−$O_t^\bullet$ bonds, 0.0097 and 0.035 eV are needed for the structural changes of $V_2O_5(SiO_2)_2O^-$ (IS9) and $V_2O_6^-$, respectively. This is also

consistent with the higher reactivity of $V_2O_5(SiO_2)_2O^-$ versus that of $V_2O_6^-$ (Figure 2). As a result, in addition to the thermodynamics and the extend of spin density localization that were realized in the previous study,[87] the reactivity of $O_t^\bullet$-containing clusters toward C−H σ bond activation also depends on the energy cost to transfer and to localize the spin densities within the clusters.

It is noticeable that the two O_t atoms with significant spin density values in $V_2O_5(SiO_2)_2O^-$/IS9 [as well as in $(V_2O_5)_2SiO_2O^-$/IS11] and $V_2O_6^-$ are in the forms of $O_t^{\bullet f}-Si-O_b-Si-O_t^{\bullet f}$ and $O_t^{\bullet f}-V-O_t^{\bullet f}$, respectively (see the note in ref 120 for notation of $O_t^{\bullet f}$). The two $O_t^{\bullet f}$ atoms in $V_2O_5SiO_2O^-$/IS2 ($O_t^{\bullet f}-Si-O_t^{\bullet f}$) is similar to the ones in $V_2O_6^-$ and the C_4H_{10} activation needs to overcome a significant overall energy barrier ($\Delta H_{0K} = 0.18$ eV for TS2, Figure 4). Therefore, it may be proposed that oxide clusters with $O_t^{\bullet f}-R-O_b-R-O_t^{\bullet f}$ structure can be more reactive than the ones with $O_t^{\bullet f}-R-O_t^{\bullet f}$.

4.3. Consideration of Active Phase versus Support for Oxide Material in Very Small Size. The $O^{-\bullet}$ radicals were suggested to be important in several surface reactions such as oxidation of methane, ethane, and benzene.[44−51] Meanwhile, it was only considered that these reactive oxygen species are involved directly with transition metal atoms. For example, the study of methane conversion to methanol and formaldehyde over vanadium oxide or molybdenum oxide supported on mesoporous silica suggested a mechanism that the reactions are initiated by the formation of $O^{-\bullet}$ coordinated with V(IV) and Mo(VI) at the surface.[48,51] However, on the basis of experimental and theoretical results in this study, we suggest that the active sites of reactive $(V_2O_5)_m(SiO_2)_nO^-$ ($m = 1$, $n = 1-4$; $m = 2$, $n = 1$) cluster anions are $Si-O_t^\bullet$ rather than $V-O_t^\bullet$ bonds. Our recent experimental and theoretical studies of the reactivity of V−Si heteronuclear oxide cluster cations $(V_2O_5)(SiO_2)_{1-4}^+$ also proposed that their active sites are $Si-O_t^\bullet$ rather than $V-O_t^\bullet$.[121] Meanwhile, the bimetallic oxide cluster $AlVO_4^+$ also has $Al-O_t^\bullet$ but not $V-O_t^\bullet$.[69] These results are in contrast with the traditional concept that transition metal oxides (such as V_2O_5) are active phase of catalysts (such as V_2O_5/SiO_2) while the main group metal or nonmetal oxides (such as SiO_2) are support materials and do not participate directly in the reaction. The heteronuclear oxides $V_2O_5(SiO_2)_{1-4}O^-$, $(V_2O_5)_2SiO_2O^-$, $V_2O_5(SiO_2)_{1-4}^+$, and $AlVO_4^+$ are with diameters ranging from 0.6 to 0.8 nm. It implies that for catalysts such as V_2O_5/SiO_2 and V_2O_5/Al_2O_3 in nanosize and further smaller regions, one should consider that the usually considered support materials (Si−O and Al−O) may well play an important role in surface reactions such as in the process of C−H activation.

5. Conclusions

The reaction of vanadium−silicon heteronuclear oxide cluster anions $V_xSi_yO_z^-$ with *n*-butane in a fast flow reactor has been studied. The $V_2O_5(SiO_2)_{1-4}O^-$ and $(V_2O_5)_2SiO_2O^-$ clusters can abstract H-atom from C_4H_{10} at room temperature, while $V_2O_6^-$ reacts much slower than these heteronuclear oxide clusters. The cluster structures and reaction mechanisms are studied by density functional calculations, and the results are in agreement with the experimental observations. The active sites of these V−Si heteronuclear oxide cluster anions are terminal oxygen atoms ($O_t^\bullet$) over which the unpaired electrons in the clusters are located. These $O_t^\bullet$ atoms are bonded with silicon ($Si-O_t^\bullet$) rather than the vanadium ($V-O_t^\bullet$) atoms. It is demonstrated that the reactivity of these $O_t^\bullet$-containing clusters including $V_2O_6^-$ toward C−H σ bond activation depends on thermodynamics, extent of spin density localization, and the energy cost to transfer and to localize the spin densities over a single O_t atom. The spin density transfer and localization are more facile in clusters with $O_t^{\bullet f}-R-O_b-R-O_t^{\bullet f}$ (R = Si) structure than in the ones with $O_t^{\bullet f}-R-O_t^{\bullet f}$ (R = Si or V).[120] The active sites of $Si-O_t^\bullet$ rather than $V-O_t^\bullet$ in the vanadium−silicon heteronuclear oxide cluster anions $V_2O_5(SiO_2)_{1-4}O^-$ and $(V_2O_5)_2SiO_2O^-$ and related cluster cations are in contrast with the concept that transition metal oxides (such as V_2O_5 in V_2O_5/SiO_2 catalyst) are the active phase of catalysts while the nonmetal oxides are support materials and do not participate directly in surface reactions.

Acknowledgment. This work was supported by the Chinese Academy of Sciences (Hundred Talents Program Fund), the National Natural Science Foundation of China (Nos. 20703048, 20803083, and 20933008), and the 973 Programs (No. 2006CB932100).

Supporting Information Available: Mass spectra for the reaction of $V_xSi_yO_z^-$ with *n*-C_4D_{10} in the selected mass region (Figure S1); DFT calculated and experimental energies of bond dissociation, vertical ionization, adiabatic electron affinity, and adiabatic or vertical electron detachments for silicon oxides and other related species (Table S1); the B3LYP optimized isomeric structures of $V_2O_5(SiO_2)_{2-4}O^-$ and $(V_2O_5)_2SiO_2O^-$ (Figures S2−S5). This material is available free of charge via the Internet at http://pubs.acs.org.

References and Notes

(1) Roithová, J.; Schröder, D. *Chem. Rev.* **2010**, *110*, 1170.
(2) Gong, Y.; Zhou, M. F. *Chem. Rev.* **2009**, *109*, 6765.
(3) Adachi, G.-y.; Imanaka, N. *Chem. Rev.* **1998**, *98*, 1479.
(4) Xue, W.; Wang, Z. C.; He, S. G.; Xie, Y.; Bernstein, E. R. *J. Am. Chem. Soc.* **2008**, *130*, 15879.
(5) Schröder, D.; Schwarz, H. *Proc. Natl. Acad. Sci.* **2008**, *105*, 18114.
(6) Xue, W.; Yin, S.; Ding, X. L.; He, S. G.; Ge, M. F. *J. Phys. Chem. A* **2009**, *113*, 5302.
(7) Ding, X. L.; Xue, W.; Ma, Y. P.; Wang, Z. C.; He, S. G. *J. Chem. Phys.* **2009**, *130*, 014303.
(8) Li, S. H.; Mirabal, A.; Demuth, J.; Wöste, L.; Siebert, T. *J. Am. Chem. Soc.* **2008**, *130*, 16832.
(9) Asmis, K. R.; Sauer, J. *Mass Spectrom. Rev.* **2007**, *26*, 542.
(10) Xie, Y.; Dong, F.; Heinbuch, S.; Rocca, J. J.; Bernstein, E. R. *Phys. Chem. Chem. Phys.* **2010**, *12*, 947.
(11) He, S. G.; Xie, Y.; Dong, F.; Heinbuch, S.; Jakubikova, E.; Rocca, J. J.; Bernstein, E. R. *J. Phys. Chem. A* **2008**, *112*, 11067.
(12) Ma, Y. P.; Xue, W.; Wang, Z. C.; Ge, M. F.; He, S. G. *J. Phys. Chem. A* **2008**, *112*, 3731.
(13) Wang, W. G.; Wang, Z. C.; Yin, S.; He, S. G.; Ge, M. F. *Chin. J. Chem. Phys.* **2007**, *20*, 412.
(14) Zemski, K. A.; Justes, D. R.; Castleman, A. W., Jr. *J. Phys. Chem. B* **2002**, *106*, 6136.
(15) Ma, J. B.; Wu, X. N.; Zhao, Y. X.; Ding, X. L.; He, S. G. *Chin. J. Chem. Phys.* **2010**, *23*, 133.
(16) The unparied electron (or spin density) in each of the $O^{-\bullet}$ containing clusters is mainly distributed over the 2p orbital(s) of one or two oxygen atoms, which is very similar to the situation of the free O^- anion system.
(17) Che, M.; Tench, A. J. *Adv. Catal.* **1982**, *31*, 77.
(18) Chiesa, M.; Giamello, E.; Che, M. *Chem. Rev.* **2010**, *110*, 1320.
(19) Dong, F.; Heinbuch, S.; Xie, Y.; Rocca, J. J.; Bernstein, E. R.; Wang, Z. C.; Deng, K.; He, S. G. *J. Am. Chem. Soc.* **2008**, *130*, 1932.
(20) Done, F.; Heinbuch, S.; Xie, Y.; Bernstein, E. R.; Rocca, J. J.; Wang, Z. C.; Ding, X. L.; He, S. G. *J. Am. Chem. Soc.* **2009**, *131*, 1057.
(21) Ma, Y. P.; Ding, X. L.; Zhao, Y. X.; He, S. G. *ChemPhysChem* **2010**, *11*, 1718.
(22) Justes, D. R.; Mitrić, R.; Moore, N. A.; Bonačić-Koutecký, V.; Castleman, A. W., Jr. *J. Am. Chem. Soc.* **2003**, *125*, 6289.
(23) Feyel, S.; Döbler, J.; Schröder, D.; Sauer, J.; Schwarz, H. *Angew. Chem., Int. Ed.* **2006**, *45*, 4681.
(24) Feyel, S.; Schröder, D.; Schwarz, H. *J. Phys. Chem. A* **2006**, *110*, 2647.
(25) Zhao, Y. X.; Wu, X. N.; Wang, Z. C.; He, S. G.; Ding, X. L. *Chem. Commun.* **2010**, *46*, 1736.
(26) Johnson, G. E.; Mitrić, R.; Tyo, E. C.; Bonačić-Koutecký, V.; Castleman, A. W., Jr. *J. Am. Chem. Soc.* **2008**, *130*, 13912.

(27) Johnson, G. E.; Tyo, E. C.; Castleman, A. W., Jr. *Proc. Natl. Acad. Sci.* **2008**, *105*, 18108.
(28) Zhao, Y. X.; Ding, X. L.; Ma, Y. P.; Wang, Z. C.; He, S. G. *Theor. Chem. Acc.* **2010**, DOI: 10.1007/s00214-010-0732-8.
(29) Johnson, G. E.; Mitrić, R.; Nössler, M.; Tyo, E. C.; Bonačić-Koutecký, V.; Castleman, A. W., Jr. *J. Am. Chem. Soc.* **2009**, *131*, 5460.
(30) Feyel, S.; Döbler, J.; Höckendorf, R.; Beyer, M. K.; Sauer, J.; Schwarz, H. *Angew. Chem., Int. Ed.* **2008**, *47*, 1946.
(31) Sierka, M.; Döbler, J.; Sauer, J.; Santambrogio, G.; Brümmer, M.; Wöste, L.; Janssens, E.; Meijer, G.; Asmis, K. R. *Angew. Chem., Int. Ed.* **2007**, *46*, 3372.
(32) Schröder, D.; Roithová, J. *Angew. Chem., Int. Ed.* **2006**, *45*, 5705.
(33) Schröder, D.; Roithová, J.; Alikhani, E.; Kwapien, K.; Sauer, J. *Chem.—Eur. J.* **2010**, *16*, 4110.
(34) De Petris, G.; Troiani, A.; Rosi, M.; Angelini, G.; Ursini, O. *Chem.—Eur. J.* **2009**, *15*, 4248.
(35) Dietl, N.; Engeser, M.; Schwarz, H. *Angew. Chem., Int. Ed.* **2009**, *48*, 4861.
(36) Harvey, J. N.; Diefenbach, M.; Schröder, D.; Schwarz, H. *Int. J. Mass Spectrom.* **1999**, *182/183*, 85.
(37) Kretzschmar, I.; Fiedler, A.; Harvey, J. N.; Schröder, D.; Schwarz, H. *J. Phys. Chem. A* **1997**, *101*, 6252.
(38) Fialko, E. F.; Kikhtenko, A. V.; Goncharov, V. B.; Zamaraev, K. I. *J. Phys. Chem. A* **1997**, *101*, 8607.
(39) Ryan, M. F.; Fiedler, A.; Schröder, D.; Schwarz, H. *J. Am. Chem. Soc.* **1995**, *117*, 2033.
(40) Schröder, D.; Fiedler, A.; Hrušák, J.; Schwarz, H. *J. Am. Chem. Soc.* **1992**, *114*, 1215.
(41) Irikura, K. K.; Beauchamp, J. L. *J. Am. Chem. Soc.* **1989**, *111*, 75.
(42) Dietl, N.; Engeser, M.; Schwarz, H. *Chem.—Eur. J.* **2009**, *15*, 11100.
(43) Dietl, N.; Engeser, M.; Schwarz, H. *Chem.—Eur. J.* **2010**, *16*, 4452.
(44) Shvets, V. A.; Kazansky, V. B. *J. Catal.* **1972**, *25*, 123.
(45) Ben, T. Y.; Lunsford, J. H. *Chem. Phys. Lett.* **1973**, *19*, 348.
(46) Ward, M. B.; Lin, M. J.; Lunsford, J. H. *J. Catal.* **1977**, *50*, 306.
(47) Parfenov, M. V.; Starokon, E. V.; Semikolenov, S. V.; Panov, G. I. *J. Catal.* **2009**, *263*, 173.
(48) Launay, H.; Loridant, S.; Nguyen, D. L.; Volodin, A. M.; Dubois, J. L.; Millet, J. M. M. *Catal. Today* **2007**, *128*, 176.
(49) Liu, R. S.; Iwamoto, M.; Lunsford, J. H. *J. Chem. Soc. Chem. Commun.* **1982**, 78.
(50) Lipatkina, N. I.; Shvets, V. A.; Kazansky, V. B. *Kinet. Katal.* **1978**, *19*, 979.
(51) Liu, H. F.; Liu, R. S.; Liew, K. Y.; Johnson, R. E.; Lunsford, J. H. *J. Am. Chem. Soc.* **1984**, *106*, 4117.
(52) Khan, M. M.; Somorjai, G. A. *J. Catal.* **1985**, *91*, 263.
(53) Zhen, K. J.; Khan, M. M.; Mak, C. H.; Lewis, K. B.; Somorjai, G. A. *J. Catal.* **1985**, *94*, 501.
(54) Lunsford, J. H. *Catal. Rev. Sci. Eng.* **1974**, *8*, 135.
(55) Cavalleri, M.; Hermann, K.; Knop-Gericke, A.; Hävecker, M.; Herbertb, R.; Hess, C.; Oestereich, A.; Dobler, J.; Schlögl, R. *J. Catal.* **2009**, *262*, 215.
(56) Nieto, J. M. L. *Top. Catal.* **2006**, *41*, 1.
(57) Bentrup, U.; Brückner, A.; Rüdinger, C.; Eberle, H. J. *Appl. Catal., A* **2004**, *269*, 237.
(58) Shah, P. R.; Baldychev, I.; Vohs, J. M.; Gorte, R. J. *Appl. Catal., A* **2009**, *361*, 13.
(59) Baron, M.; Abbott, H.; Bondarchuk, O.; Stacchiola, D.; Uhl, A.; Shaikhutdinov, S.; Freund, H. J.; Popa, C.; Ganduglia-Pirovano, M. V.; Sauer, J. *Angew. Chem., Int. Ed.* **2009**, *48*, 8006.
(60) Nguyen, L. D.; Loridant, S.; Launay, H.; Pigamo, A.; Dubois, J. L.; Millet, J. M. M. *J. Catal.* **2006**, *237*, 38.
(61) Čapek, L.; Bulánek, R.; Adam, J.; Smoláková, L.; Sheng, Y. H.; Čičmanec, P. *Catal. Today* **2009**, *141*, 282.
(62) Murgia, V.; Torres, E. M. F.; Gottifredi, J. C.; Sham, E. L. *Appl. Catal., A* **2006**, *312*, 134.
(63) Kin, T.; Wachs, I. E. *J. Catal.* **2008**, *255*, 197.
(64) Chimentao, R. J.; Herrera, J. E.; Kwak, J. H.; Medina, F.; Wang, Y.; Peden, C. H. F. *Appl. Catal., A* **2007**, *332*, 263.
(65) Gregori, F.; Nobili, I.; Bigi, F.; Maggi, R.; Predieri, G.; Sartori, G. *J. Mol. Catal. A: Chem.* **2008**, *286*, 124.
(66) Zhao, C. L.; Wachs, I. E. *J. Catal.* **2008**, *257*, 181.
(67) Fielicke, A.; Rademann, K. *Chem. Phys. Lett.* **2002**, *359*, 360.
(68) Nöβer, M.; Mitrić, R.; Bonačić-Koutecký, V.; Johnson, G. E.; Tyo, E. C.; Castleman, A. W., Jr. *Angew. Chem., Int. Ed.* **2010**, *49*, 407.
(69) Wang, Z. C.; Wu, X. N.; Zhao, Y. X.; Ma, J. B.; Ding, X. L.; He, S. G. *Chem. Phys. Lett.* **2010**, *489*, 25.
(70) Janssens, E.; Santambrogio, G.; Brümmer, M.; Wöste, L.; Lievens, P.; Sauer, J.; Meijer, G.; Asmis, K. R. *Phys. Rev. Lett.* **2006**, *96*, 233401.
(71) Zemski, K. A.; Justes, D. R.; Castleman, A. W., Jr. *J. Phys. Chem. A* **2001**, *105*, 10237.
(72) Bell, R. C.; Castleman, A. W., Jr. *J. Phys. Chem. A* **2002**, *106*, 9893.
(73) Rozanska, X.; Sauer, J. *J. Phys. Chem. A* **2009**, *113*, 11586.
(74) Bell, R. C.; Zemski, K. A.; Kerns, K. P.; Deng, H. T.; Castleman, A. W., Jr. *J. Phys. Chem. A.* **1998**, *102*, 1733.
(75) Fielicke, A.; Rademann, K. *Phys. Chem. Chem. Phys.* **2002**, *4*, 2621.
(76) Zemski, K. A.; Justes, D. R.; Bell, R. C.; Castleman, A. W., Jr. *J. Phys. Chem. A* **2001**, *105*, 4410.
(77) Zhai, H. J.; Döbler, J.; Sauer, J.; Wang, L. S. *J. Am. Chem. Soc.* **2007**, *129*, 13270.
(78) Wu, H. B.; Wang, L. S. *J. Chem. Phys.* **1998**, *108*, 5310.
(79) Santambrogio, G.; Brümmer, M.; Wöste, L.; Döbler, J.; Sierka, M.; Sauer, J.; Meijer, G.; Asmis, K. R. *Phys. Chem. Chem. Phys.* **2008**, *10*, 3992.
(80) Feyel, S.; Schwarz, H.; Schröer, D.; Daniel, C.; Hartl, H.; Döbler, J.; Sauer, J.; Santambrogio, G.; Wöste, L.; Asmis, K. R. *ChemPhysChem* **2007**, *8*, 1640.
(81) Asmis, K. R.; Santambrogio, G.; Brümmer, M.; Sauer, J. *Angew. Chem.* **2005**, *117*, 3182.
(82) Bell, R. C.; Zemski, K. A.; Justes, D. R.; Castleman, A. W., Jr. *J. Chem. Phys.* **2001**, *114*, 798.
(83) Vyboishchikov, S. F.; Sauer, J. *J. Phys. Chem. A* **2000**, *104*, 10913.
(84) Li, S. H.; Mirabal, A.; Demuth, J.; Wöste, L.; Siebert, T. *J. Am. Chem. Soc.* **2008**, *130*, 16832.
(85) Li, H. B.; Tian, S. X.; Yang, J. L. *Chem.—Eur. J.* **2009**, *15*, 10747.
(86) Waters, T.; Khairallah, G. N.; Wimala, S. A. S. Y.; Ang, Y. C.; O'Hair, R. A. J.; Wedd, A. G. *Chem. Commun.* **2006**, 4503.
(87) Wu, X. N.; Zhao, Y. X.; Xue, W.; Wang, Z. C.; He, S. G.; Ding, X. L. *Phys. Chem. Chem. Phys.* **2010**, *12*, 3984.
(88) Waters, T.; O'Hair, R. A. J.; Wedd, A. G. *J. Am. Chem. Soc.* **2003**, *125*, 3384.
(89) O'Hair, R. A. J. *Chem. Commun.* **2006**, 1469.
(90) Geusic, M. E.; Morse, M. D.; O'Brien, S. C.; Smalley, R. E. *Rev. Sci. Instrum.* **1985**, *56*, 2123.
(91) Frisch, M. J.; Trucks, G. W.; Schlegel, H. B.; Scuseria, G. E.; Robb, M. A.; Cheeseman, J. R.; Montgomery, J. A., Jr.; Vreven, T.; Kudin, K. N.; Burant, J. C.; Millam, J. M.; Iyengar, S. S.; Tomasi, J.; Barone, V.; Mennucci, B.; Cossi, M.; Scalmani, G.; Rega, N.; Petersson, G. A.; Nakatsuji, H.; Hada, M.; Ehara, M.; Toyota, K.; Fukuda, R.; Hasegawa, J.; Ishida, M.; Nakajima, T.; Honda, Y.; Kitao, O.; Nakai, H.; Klene, M.; Li, X.; Knox, J. E.; Hratchian, H. P.; Cross, J. B.; Bakken, V.; Adamo, C.; Jaramillo, J.; Gomperts, R.; Stratmann, R. E.; Yazyev, O.; Austin, A. J.; Cammi, R.; Pomelli, C.; Ochterski, J. W.; Ayala, P. Y.; Morokuma, K.; Voth, G. A.; Salvador, P.; Dannenberg, J. J.; Zakrzewski, V. G.; Dapprich, S.; Daniels, A. D.; Strain, M. C.; Farkas, O.; Malick, D. K.; Rabuck, A. D.; Raghavachari, K.; Foresman, J. B.; Ortiz, J. V.; Cui, Q.; Baboul, A. G.; Clifford, S.; Cioslowski, J.; Stefanov, B. B.; Liu, G.; Liashenko, A.; Piskorz, P.; Komaromi, I.; Martin, R. L.; Fox, D. J.; Keith, T.; Al-Laham, M. A.; Peng, C. Y.; Nanayakkara, A.; Challacombe, M.; Gill, P. M. W.; Johnson, B.; Chen, W.; Wong, M. W.; Gonzalez, C.; Pople, J. A. *Gaussian 03*, revision B.05; Gaussian, Inc.: Wallingford, CT, 2003.
(92) Glendening, E. D.; Reed, A. E.; Carpenter, J. E.; Weinhold, F. NBO, version 3.1.
(93) Schlegel, H. B. *J. Comput. Chem.* **1982**, *3*, 214.
(94) Gonzalez, C.; Schlegel, H. B. *J. Chem. Phys.* **1989**, *90*, 2154.
(95) Gonzalez, C.; Schlegel, H. B. *J. Phys. Chem.* **1990**, *94*, 5523.
(96) Becke, A. D. *Phys. Rev. A* **1988**, *38*, 3098.
(97) Becke, A. D. *J. Chem. Phys.* **1993**, *98*, 5648.
(98) Lee, C.; Yang, W.; Parr, R. G. *Phys. Rev. B* **1988**, *37*, 785.
(99) Schäfer, A.; Huber, C.; Ahlrichs, R. *J. Chem. Phys.* **1994**, *100*, 5829.
(100) Boys, S. F.; Bernardi, F. *Mol. Phys.* **1970**, *19*, 553.
(101) Simon, S.; Duran, M.; Dannenberg, J. J. *J. Chem. Phys.* **1996**, *105*, 11024.
(102) Wang, Z. C.; Xue, W.; Ma, Y. P.; Ding, X. L.; He, S. G.; Dong, F.; Heinbuch, S.; Rocca, J. J.; Bernstein, E. R. *J. Phys. Chem. A* **2008**, *112*, 5984.
(103) Wang, Z. C.; Ding, X. L.; Ma, Y. P.; Cao, H.; Wu, X. N.; Zhao, Y. X.; He, S. G. *Chin. Sci. Bull.* **2009**, *54*, 2814.
(104) Ding, X. L.; Xue, W.; Ma, Y. P.; Zhao, Y. X.; Wu, X. N.; He, S. G. *J. Phys. Chem. C* **2010**, *114*, 3161.
(105) Rozanska, X.; Fortrie, R.; Sauer, J. *J. Phys. Chem. C* **2007**, *111*, 6041.
(106) Döbler, J.; Pritzsche, M.; Sauer, J. *J. Phys. Chem. C* **2009**, *113*, 12454.
(107) Rozanska, X.; Sauer, J. *Int. J. Quantum Chem.* **2008**, *108*, 2223.
(108) Sauer, J.; Döbler, J. *Dalton Trans.* **2004**, 3116.
(109) Lu, W. C.; Wang, C. Z.; Nguyen, V.; Schmidt, M. W.; Gordon, M. S.; Ho, K. M. *J. Phys. Chem. A* **2003**, *107*, 6936.
(110) Nakagawa, H.; Asano, M.; Kubo, K. *J. Nucl. Mater.* **1981**, *102*, 292.
(111) Kostko, O.; Ahmed, M. *J. Phys. Chem. A* **2009**, *113*, 1225.

(112) Wang, L. S.; Wu, H. B.; Desai, S. R.; Fan, J. W.; Colson, S. D. *J. Phys. Chem.* **1996**, *100*, 8697.

(113) Hunter, E. P.; Lias, S. G. *J. Phys. Chem. Ref. Data* **1998**, *27*, 413.

(114) Gutsev, G. L.; Andrews, L.; Bauschlicher, C. W., Jr. *Theor. Chem. Acc.* **2003**, *109*, 298.

(115) Nakao, Y.; Hirao, K.; Taketsugu, T. *J. Chem. Phys.* **2001**, *114*, 8.

(116) Bande, A.; Lüchow, A. *Phys. Chem. Chem. Phys.* **2008**, *10*, 3371.

(117) Pedley, J. B.; Marshall, E. M. *J. Phys. Chem. Ref. Data* **1983**, *12*, 967.

(118) http://physics.nist.gov/PhysRefData/Compositions/index.html.

(119) Wu, X. N.; Zhao, Y. X.; He, S. G.; Ding, X. L. *Chin. J. Chem. Phys.* **2009**, *22*, 635.

(120) To differentiate from normal notations of oxygen-centered biradicals such as $O_t^{\bullet}-Si-O_b-Si-O_t^{\bullet}$ and $O_t^{\bullet}-V-O_t^{\bullet}$, the symbol $O_t^{\bullet f}$ is used to denote the O_t atom with only a faction of the spin density values [for example, the O_t atoms with a spin density of $\sim$0.5 |e| in $V_2O_5(SiO_2)_2O^-$].

(121) Ding, X. L.; Zhao, Y. X.; Wu, X. N.; Wang, Z. C.; Ma, J. B.; He, S. G. Hydrogen-Atom Abstraction from Methane by Stoichiometric Vanadium-Silicon Heteronuclear Oxide Cluster Cations. *Chem.—Eur. J.* **2010**, accepted for publication.

JP1045244